

Quantum phase transition of two-level atoms interacting with a finite radiation field

L. F. Quezada,^{1, 2,*} A. Martín-Ruiz,^{1, 2, †} and A. Frank^{1, 2, 3, ‡}

¹*Instituto de Ciencias Nucleares, Universidad Nacional Autónoma de México, 04510 Ciudad de México, México*
²*Centro de Ciencias de la Complejidad, Universidad Nacional Autónoma de México, 04510 Ciudad de México, México*
³*El Colegio Nacional, Ciudad de México, México*

We introduce a group-theoretical extension of the Dicke model which describes an ensemble of two-level atoms interacting with a finite radiation field. The latter is described by a spin model which exhibits the main properties of the Kerr medium, and whose main feature is that it possesses a maximum number of excitations. We use the energy surface minimization method to demonstrate that the extended Dicke model exhibits a quantum phase transition, and we analyse its dependence upon the maximum number of excitations of the model. Our analysis is carried out via three methods: through mean-field analysis (i.e. by using the tensor product of coherent states), by using parity-preserving symmetry-adapted states (using the critical values obtained in the mean-field analysis and numerically minimizing the energy surface) and by means of the exact quantum solution (i.e. by numerically diagonalizing the Hamiltonian). Possible connections with the qp -deformed algebras are also discussed.

I. INTRODUCTION

One of the most important problems of relativistic quantum field theories (QFTs) are the ultraviolet (UV) divergences that typically plague perturbative expansions. Most of the existing regularization techniques require severe mutilation of the logical foundations of the theory [1]. For example, Pauli-Villars and Lorentz-invariant higher-derivative regularizations violate unitarity. In general, perturbative expansions of QFTs are described by free fields in which quantum excitations are constructed in terms of bosonic or fermionic oscillators. In the bosonic case, the resulting Hilbert space is infinite-dimensional basically due to the presence of continuum quantum numbers such as the momentum (which ranges between $-\infty$ and $+\infty$). This specific property is that leads to the typical UV divergences. Therefore, the construction of a QFT with a maximum number of excitations (i.e. with a maximal energy and momentum) could alleviate the UV problem. This article is a first attempt on this problem via a group-theoretical approach. However, although the final purpose is the construction of a QFT free from UV divergences, here we shall explore the physical implications of a natural extension of the fundamental Lie group describing bosonic excitations on a simple yet realistic quantum-optical model.

The Dicke model (DM) describes a single bosonic mode interacting collectively with a set of N two-level systems (e.g. a cold two-level atomic cloud). An important feature of this model is the presence of a phase transition between the normal and the superradiant behaviour [3–5], which is indeed sensitive to the properties of the bosonic field. The Dicke quantum phase transition has recently been observed in a superfluid gas in an optical

cavity [6, 7]. Although this development was achieved using time-dependent fields dressing the system, the recent progress in the technology of trapped-atom lasers and cavity quantum electrodynamics (QED) experiments serve as a test bed for this model and its many extensions. This is precisely what motivates the model we shall introduce, since these experiments could help to understand the key features of the radiation field coupled to the system of atoms. In this sense, the physics of a set of N two-level atoms interacting with a finite radiation field should exhibit some aspects about the maximal number of quantum excitations allowed in the system. In particular, the expectation value of the number of photons and the critical point where the quantum phase transition takes place should be sensitive to the new radiation field. In this paper we conduct only a theoretical analysis of our model, and we do not intent to propose an experiment to test it.

Quantum algebras [8] have already found applications in conformal field theory and quantum gravity, in the description of spin chains, and in the nuclear and molecular spectroscopy. They can be understood as deformations of the usual Lie algebras giving rise to the concept of qp -deformed bosons. In quantum optics many authors have studied the q -deformed Jaynes-Cummings (JC) and Dicke models, which are obtained by replacing the usual creation and annihilation bosonic operators by their corresponding qp -deformed operators [9–13]. Different choices of the deformation function yield to different models and hence to new physics. Despite their mathematical richness, these models mutilate the basic algebraic structure of the quantum-optical models.

In this paper we introduce a group-theoretical extension of the Dicke model which is based on the fact that the Heisenberg-Weyl algebra $HW(1)$ describing the usual bosonic mode can be obtained by contraction of the $SU(2)$ algebra [14]. In short we propose a spin model which exhibits the main properties of the Kerr medium. This model is formulated in terms of spin operators K_i acting on the $(2k + 1)$ -dimensional Hilbert space of a

*Electronic address: luis.fernando@correo.nucleares.unam.mx

†Electronic address: alberto.martin@nucleares.unam.mx

‡Electronic address: frank@nucleares.unam.mx

particle with spin k . In a definite unitary irreducible representation k , we built creation and annihilation operators which contract to the usual HW(1) bosonic operators in the large k -representation limit. The corresponding SU(2) harmonic oscillator exhibits a maximum number of excitations $2k$ (which is a consequence of the corresponding algebra) and hence the energy spectrum is bounded from above [15]. From now on we will refer to this model as the $SU(2) \otimes SU(2)$ Dicke model, the k -Dicke model, or in short the k DM. From the quantum field theoretical perspective, our k -oscillator model may have significant consequences in the case of a scalar field theory: a natural cutoff for the momenta. In this paper, however, we focus on the effects of our algebraic model upon the phase transition and the expectation values of the physically measurable quantities in the Dicke model, and we left the construction of the k -QFT for future investigations. From the quantum-optical perspective, the k DM would be interesting since current circuit QED architectures allow the engineering of a wide range of Kerr-type non-linearities, including the one presented in this work. This provides a platform in which the finite oscillator model can be tested.

The paper is organized as follows. After a brief review of the Dicke model in Sec. II A we present our algebraic model in Sec. II B. The k -Dicke model is introduced in Sec. II C. Using the suitable coherent states, in Sec. III we perform a mean field analysis of the phase transition and compare the obtained results with the large k -representation limit. In Sec. IV we construct parity preserving coherent states (which is possible due to the parity symmetry of the k D Hamiltonian) to analyze the phase transition. We find that they represent a good approximation to the exact quantum solution of the ground state of the model, which is discussed in Sec. V. Possible connections with the qp -deformed algebras are briefly discussed in the concluding section VI.

II. MODEL HAMILTONIAN

A. The Dicke model

The Dicke Hamiltonian describes N two-level identical atoms, with energy separation ω_A , interacting collectively with a one-mode radiation field of frequency Ω . In the dipolar approximation, the Hamiltonian (with $\hbar = 1$) reads [2]

$$H_D = \omega_A J_z + \Omega a^\dagger a - \frac{2\gamma}{\sqrt{N}} J_x (a + a^\dagger), \quad (1)$$

where γ is the atom-field interaction strength, the collective pseudo-spin operators $J_i = \sum_{n=1}^N S_i^{(n)}$, with $S_i = \sigma_i/2$ (being σ_i the Pauli matrices), satisfy the SU(2) commutation relations

$$[J_+, J_-] = 2J_z, \quad [J_z, J_\pm] = \pm J_\pm, \quad (2)$$

and act on a $(2j + 1)$ -dimensional Hilbert space generated by the Dicke states $\{|j, m_j\rangle\}$, which are common eigenstates of the commuting observables J^2 and J_z , with eigenvalues $j(j + 1)$ and m_j , respectively. For the electromagnetic field the creation and annihilation operators a^\dagger and a , appearing in the Hamiltonian (1), satisfy the commutation relations of the Lie algebra generators of the Heisenberg-Weyl group HW(1), i.e.

$$[a, a^\dagger] = 1, \quad [a, n] = a, \quad [a^\dagger, n] = -a^\dagger, \quad (3)$$

where $n = a^\dagger a$ is the photon number operator, which acts on an infinite-dimensional Hilbert space generated by the states $\{|n\rangle\}$, with n denoting its corresponding eigenvalue. The Dicke Hamiltonian (1) undergoes a quantum phase transition at a critical value of the atom-field coupling strength $\gamma_c^D = \sqrt{\omega_A N \Omega / 8j}$, where the system transits from a normal phase ($\gamma < \gamma_c^D$) to a super-radiant phase ($\gamma > \gamma_c^D$) [3–5].

B. Algebraic model

It is well known that the HW(1) algebra can be obtained by contraction of the SU(2) algebra. Here, we consider a new set of pseudo-spin operators $\{K_i\}$ satisfying the SU(2) commutation relations

$$[K_+, K_-] = 2K_z, \quad [K_z, K_\pm] = \pm K_\pm, \quad (4)$$

and, in a definite unitary irreducible representation k , we build the operators

$$b_k = \frac{K_-}{\sqrt{2k}}, \quad b_k^\dagger = \frac{K_+}{\sqrt{2k}}, \quad n_k = K_z + k, \quad (5)$$

which act on a $(2k + 1)$ -dimensional Hilbert space of a particle with spin k [15]. In this representation, the SU(2) algebra (4) becomes

$$[b_k, b_k^\dagger] = 1 - \frac{n_k}{k}, \quad [b_k, n_k] = b_k, \quad [b_k^\dagger, n_k] = -b_k^\dagger, \quad (6)$$

which allows the interpretation of b_k and b_k^\dagger as the annihilation and creation operators for the quanta labeled by the number operator n_k . Note that the commutator between the deformed ladder operators ceases to be a c -number.

Now we introduce the k -oscillator model, which is a quantum system characterized by an algebraic Hamiltonian of the form

$$H_k = \frac{\Omega}{2} (b_k b_k^\dagger + b_k^\dagger b_k), \quad (7)$$

where Ω is a constant. With the help of the algebra (6), the aforesaid Hamiltonian can equivalently be cast in terms of the number operator as

$$H_k = \Omega \left(n_k + \frac{1}{2} - \frac{n_k^2}{2k} \right). \quad (8)$$

Note that, in contrast to the harmonic oscillator case, the k -oscillator is no longer a linear function of the number operator. In the limit $k \rightarrow \infty$, the k -algebra (6) contracts to the HW(1) algebra (3), and the nonlinear term in the Hamiltonian (8) disappears.

The analogy between the k -oscillator (8) and the usual Kerr Hamiltonian $H_K = \Omega(n+1/2) - \chi n^2$ is evident, since the spin excitation number operator n_k has non-negative integer spectrum. The main difference between the photon number operator and the spin excitation number operator is that the latter is bounded from above: $n_k \leq 2k$. This result implies that the k -oscillator possesses a maximum energy given by $E_{k \text{ max}} = (\omega/2)(k+1)$. This result is the one that may have significant consequences in the case of a scalar field theory: a natural cutoff for the momenta. Notice that the harmonic-oscillator properties are retrieved in the limit $k \rightarrow \infty$: H_k becomes the usual bosonic oscillator, the spin number of excitations is unbounded and the maximal energy goes to infinity.

C. The k -Dicke model

Having defined in the preceding section a suitable algebraic model for a harmonic oscillator with a maximum number of excitations, now let us generalize the Dicke model by writing the Hamiltonian in the following form:

$$H_{kD} = \omega_A J_z + \frac{\Omega}{2k} (K^2 - K_z^2) - \frac{4\gamma}{\sqrt{2kN}} J_x K_x, \quad (9)$$

which manifests now that the dynamical algebra is $SU(2) \otimes SU(2)$. From now on we refer to this model as the k -Dicke model or simply as k -DM. As in the Dicke Hamiltonian (1), the first term is the energy operator for the atoms. The second term corresponds to the energy operator for the field, which in this case corresponds to the model Hamiltonian (8) expressed in terms of the $\{K_i\}$ pseudo-spin operators. In the dipole approximation, the coupling between the ensemble of atoms and the finite radiation field is given by the last term above. One can further see that the Hamiltonian H_{kD} reduces to $H_D + \Omega/2$ under the group contraction (i.e. in the limit $k \rightarrow \infty$), as it should be. Also, the Hamiltonian (9) commutes with the operators J^2 and K^2 . Consequently, it connects only states with the same total spins j and k , i.e. that belong to the same Dicke manifold. Let us keep k finite and investigate the physical properties of the extended Dicke model (9).

It is worth underlying that in a foregoing investigation we introduced the k -extended Jaynes-Cumming model (in the dipole and rotating wave approximations), which remains exactly solvable with the new $SU(2) \otimes SU(2)$ dynamical algebra [16]. There we showed that the temporal evolution of both the atomic and field quantum properties (e.g. collapses and revivals, photon anti-bunching and squeezing) exhibit significant different behavior from that of the usual JC model for small values of k . In a similar vein, in this article we study the quantum phase

transition in the k -Dicke model by using the energy surface minimization method, which consists of minimizing the surface that is obtained by taking the expectation value of the Hamiltonian (9) with respect to some trial variational state. This method has been extensively used to study the phase transition in the Dicke model [17–22] as well as in more general models using three-level systems [23–27]. Of course, the success of the method depends on the choice of the trial state used to model the ground state of the system. We first perform a mean field analysis by using the tensor product of the coherent states in each subspace as a trial state. Next, we employ the symmetry-adapted states, which are parity-preserving trial states obtained by projecting the tensor product of coherent states. Finally, we obtain the exact quantum solution by numerically diagonalizing the Hamiltonian (9).

III. MEAN FIELD ANALYSIS

In order to obtain an energy surface, we first use as a trial state the direct product of coherent states in each subspace. For the particle sector, we use the standard $SU(2)$ spin states [28], i.e.

$$|\xi\rangle = \frac{1}{(1+|\xi|^2)^j} \sum_{m_j=0}^{2j} \binom{2j}{m_j}^{1/2} \xi^{m_j} |j, m_j - j\rangle, \quad (10)$$

where $\xi = \tan(\theta/2)e^{i\phi}$, and $|j, m_j\rangle$ is a Dicke state. The angles $\theta \in [0, \pi)$ and $\phi \in [0, 2\pi)$ determine a point on the Bloch sphere. In the problem at hand, the radiation field is modeled by the k -oscillator, and thus we use the $SU(2)$ spin coherent state,

$$|\eta\rangle = \frac{1}{(1+|\eta|^2)^k} \sum_{m_k=0}^{2k} \binom{2k}{m_k}^{1/2} \eta^{m_k} |k, m_k - k\rangle, \quad (11)$$

for the photon sector, which contracts to the Heisenberg-Weyl coherent state $|\alpha\rangle$ in the large k -representation limit [16, 29]. Here, $\eta = \tan(\psi/2)e^{i\varphi}$, $\psi \in [0, \pi)$ and $\varphi \in [0, 2\pi)$. The trial state $|\Psi\rangle = |\xi\rangle \otimes |\eta\rangle$ contains N particles and up to $2k$ photons distributed in all possible ways between the two levels.

The expectation value of the k -Dicke Hamiltonian in this trial state is defined as the energy surface, i.e. $E_k^{\text{MF}}(\vec{\lambda}) = \langle \Psi | H | \Psi \rangle = \langle H \rangle^{\text{MF}}$, where $\vec{\lambda} = (\theta, \phi, \psi, \varphi)$. The superscript MF indicates that the expectation value is calculated in the state $|\Psi\rangle$, within the mean field analysis. Straightforward calculations show that the energy surface can be written in the simple form

$$E_k^{\text{MF}}(\vec{\lambda}) = \omega_A \mathcal{J}_k^{\text{MF}}(\vec{\lambda}) + \Omega \left(\nu_k^{\text{MF}}(\vec{\lambda}) + \frac{1}{2} \right) + \gamma \mathcal{I}_k^{\text{MF}}(\vec{\lambda}), \quad (12)$$

where

$$\mathcal{J}_k^{\text{MF}}(\vec{\lambda}) \equiv \langle J_z \rangle^{\text{MF}} = -j \cos \theta \quad (13)$$

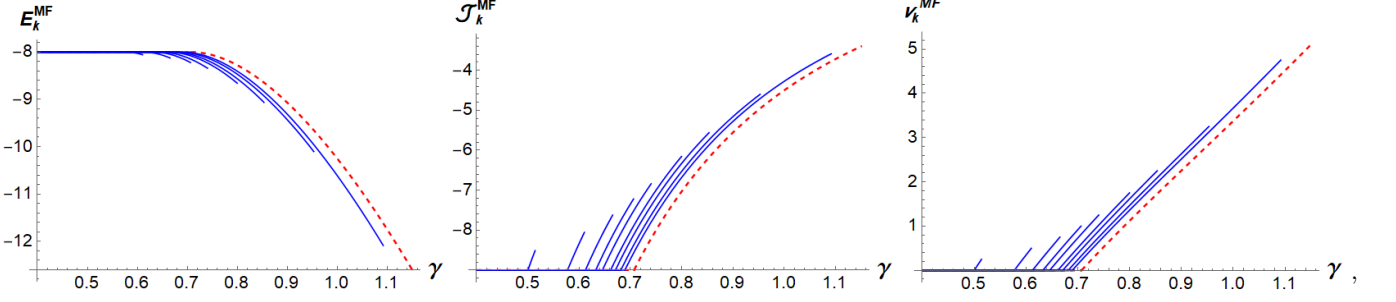


FIG. 1: Plot of the ground-state energy E_k^{MF} (left), the expectation value of the atomic relative population operator $\mathcal{J}_k^{\text{MF}}$ (center) and the expectation value of the analogue of the photon number operator ν_k^{MF} (right), as function of the field-matter coupling γ for $k \in \{1, \frac{3}{2}, 2, \frac{5}{2}, 3, 4, 5, 7, 10\}$ (blue-continuous lines). As a benchmark, the red-dashed lines show these same quantities in the limiting case $k \rightarrow \infty$, which corresponds to the $\text{HW}(1) \otimes \text{SU}(2)$ Dicke model. All plots were obtained using $\omega_A = 1$, $\Omega = 2$, $N = 18$ and $j = 9$.

is the expectation value of the atomic relative population operator,

$$\begin{aligned} \mathcal{I}_k^{\text{MF}}(\vec{\lambda}) &\equiv -\frac{4}{\sqrt{2kN}} \langle J_x K_x \rangle^{\text{MF}} \\ &= -2j\sqrt{\frac{2k}{N}} \sin \theta \sin \psi \cos \phi \cos \varphi \end{aligned} \quad (14)$$

is the expectation value of the interaction term in Hamiltonian (9), and

$$\nu_k^{\text{MF}}(\vec{\lambda}) \equiv \left\langle \frac{H_k}{\Omega} - \frac{1}{2} \right\rangle^{\text{MF}} = \frac{1}{2}(k - 1/2) \sin^2 \psi. \quad (15)$$

Notice that $\nu_k^{\text{MF}}(\vec{\lambda})$ is defined dividing the total energy of the radiation field in equal chunks of energy Ω and then subtracting the zero-point energy, which is clearly different from $\langle n_k \rangle^{\text{MF}}$ with n_k as in equation (5). Indeed one can further verify that $\nu_k^{\text{MF}} = \langle n_k \rangle^{\text{MF}} - \frac{1}{2k} \langle n_k^2 \rangle^{\text{MF}}$, as it should be. The motivation behind the definition of ν_k^{MF} is only to maintain a close analogy with the expectation value of the photon number operator in the usual Dicke model, although they are physically different. In Sec. IV, where the total excitation number operator is required to construct symmetry-adapted states, we use certainly the number operator n_k which correctly closes the $\text{SU}(2)$ algebra.

The critical points $\vec{\lambda}_c^{\text{MF}}$ of the energy surface (12) are obtained by equating its first derivative to zero, i.e.

$$\frac{\partial E_k^{\text{MF}}(\vec{\lambda})}{\partial \vec{\lambda}} \Big|_{\vec{\lambda}=\vec{\lambda}_c^{\text{MF}}} = \vec{0}. \quad (16)$$

Those which correspond to minima in the energy surface are

$$\vec{\lambda}_1^{\text{MF}} = (0, \phi_0, 0, \varphi_0), \quad \text{for } |\gamma| < \gamma_c, \quad (17)$$

being ϕ_0 and φ_0 arbitrary azimuthal angles; and

$$\vec{\lambda}_2^{\text{MF}} = (\theta_c, \phi_c, \psi_c, \varphi_c), \quad \text{for } \gamma_c < |\gamma| < \gamma_m, \quad (18)$$

where

$$\theta_c = \arccos(\gamma_c/\gamma)^2, \quad (19)$$

$$\psi_c = \arcsin \left[\frac{\omega_A \gamma \mu}{2\gamma_c^2} \sqrt{\frac{N}{2k}} \sqrt{1 - (\gamma_c/\gamma)^4} \right], \quad (20)$$

with $\mu \equiv \cos \varphi_c \cos \phi_c = \pm 1$. There are four solutions to the later condition in the domain $[0, 2\pi) \times [0, 2\pi)$. They are $(0, 0)$, (π, π) , $(0, \pi)$ and $(\pi, 0)$, with the notation (ϕ_c, φ_c) . In this paper we focus on the case for which $\mu = 1$. In eqs. (19) and (20), we have defined the critical value of the field-matter coupling,

$$\gamma_c = \sqrt{\frac{\omega_A N \Omega (k - 1/2)}{8jk}}, \quad (21)$$

at which a phase transition occurs, and from the fact that $\max(\sin \psi_c) = 1$ in the domain $[0, \pi)$ we obtain a cut-off value for the coupling

$$\gamma_m = \gamma_c \sqrt{\frac{\Omega(k - 1/2)}{2\omega_A j} + \sqrt{1 + \left[\frac{\Omega(k - 1/2)}{2\omega_A j} \right]^2}}, \quad (22)$$

which is a direct consequence of the maximum number of excitations of the k -oscillator. The condition $|\gamma| < \gamma_c$ defines the normal phase (where the ground state has zero photons and no excited atoms) and the condition $\gamma_c < |\gamma| < \gamma_m$ describes the super-radiant phase. As we shall see below, a phase transition occurs at $\gamma = \gamma_c$. Note that, as expected, the large k -representation limit ($k \rightarrow \infty$) leads to $\gamma_c \rightarrow \gamma_c^D = \sqrt{\omega_A N \Omega / 8j}$ (the critical value of the usual Dicke model) and $\gamma_m \rightarrow \infty$ (unbounded number of photons).

Substituting the critical points $\vec{\lambda}_1^{\text{MF}}$ and $\vec{\lambda}_2^{\text{MF}}$ into eq. (12) we obtain the energy of the coherent ground state as a function of the Hamiltonian parameters,

$$E_k^{\text{MF}}(\gamma) = \begin{cases} \frac{\Omega}{2} - j\omega_A, & \text{for } |\gamma| < \gamma_c \\ \frac{\Omega}{2} - \frac{j\omega_A}{2} \left[(\gamma/\gamma_c)^2 + (\gamma_c/\gamma)^2 \right], & \text{for } \gamma_c < |\gamma| < \gamma_m \end{cases}. \quad (23)$$

In a similar fashion, we can also obtain that the expectation values of the atomic relative population operator and the photon number operator can be written as

$$\mathcal{J}_k^{\text{MF}}(\gamma) = \begin{cases} -j, & \text{for } |\gamma| < \gamma_c \\ -j(\gamma_c/\gamma)^2, & \text{for } \gamma_c < |\gamma| < \gamma_m \end{cases}, \quad (24)$$

and

$$\nu_k^{\text{MF}}(\gamma) = \begin{cases} 0, & \text{for } |\gamma| < \gamma_c \\ \frac{j\omega_A}{2\Omega} [(\gamma/\gamma_c)^2 - (\gamma_c/\gamma)^2], & \text{for } \gamma_c < |\gamma| < \gamma_m \end{cases}. \quad (25)$$

respectively. In Fig. 1 we show the ground-state energy E_k^{MF} (at left), the expectation values of the atomic relative population operator $\mathcal{J}_k^{\text{MF}}$ (at center) and the photon number operator ν_k^{MF} (at right), as a function of the field-matter coupling γ for $N = 2j = 18$ and $k \in \{1, \frac{3}{2}, 2, \frac{5}{2}, 3, 4, 5, 7, 10\}$. As a benchmark, the red-dashed lines show these same quantities for the archetypal Dicke model. We observe that the energy, atomic population and photon number in the k -Dicke model, approaches asymptotically to the usual results for the $\text{HW}(1) \otimes \text{SU}(2)$ Dicke model as increasing k , as expected. For small values of k , we observe significant departures from the usual results mainly because both the critical value γ_c and the cutoff value γ_m of the field-matter coupling decreases. As we will show below, the same curves are obtained for symmetry-adapted variational states as well as for exact quantum solutions.

IV. SYMMETRY-ADAPTED STATES ANALYSIS

The k -Dicke Hamiltonian (9) has a parity symmetry given by

$$[e^{i\pi\Lambda}, H_{kD}] = 0, \quad (26)$$

where

$$\Lambda = \sqrt{J^2 + \frac{1}{4}} - \frac{1}{2} + J_z + \sqrt{K^2 + \frac{1}{4}} - \frac{1}{2} + K_z \quad (27)$$

is the excitation number operator with eigenvalues $\lambda = j + m_j + k + m_k$. This allows for the classification of the eigenstates of H_{kD} in terms of the parity of the eigenvalues λ . We observe that the set of $\text{SU}(2)$ coherent states $\{|\xi\rangle, |\eta\rangle\}$ strongly mixes states with different parity. Therefore, we can build up symmetry-adapted coherent states that preserve the symmetry of the k -Dicke Hamiltonian, by acting with the projectors of the symmetric and anti-symmetric representations of the cyclic group C_2 [30]

$$\mathcal{P}_{\pm} = \frac{1}{2} (I \pm e^{i\pi\Lambda}), \quad (28)$$

upon the state $|\Psi\rangle = |\xi\rangle \otimes |\eta\rangle$. Explicitly we have

$$\begin{aligned} |\xi, \eta\rangle_{\pm} &= \mathcal{N}_{\pm} \mathcal{P}_{\pm} |\xi\rangle \otimes |\eta\rangle \\ &= \mathcal{N}_{\pm} (|\xi\rangle \otimes |\eta\rangle \pm |-\xi\rangle \otimes |-\eta\rangle), \end{aligned} \quad (29)$$

where the normalization factor for the even (+) and odd (-) states are

$$\mathcal{N}_{\pm}(\theta, \psi) = \left[2 \pm 2 (-\cos \theta)^{2j} (-\cos \psi)^{2k} \right]^{-1/2}. \quad (30)$$

Now we perform a variational analysis of the problem by using the symmetry-adapted coherent states (29) as a trial state. As before, the energy surface is defined as the expectation value of the k -Dicke Hamiltonian in the state $|\xi, \eta\rangle_{\pm}$, i.e. $E_{k, \pm}^{\text{SAS}}(\vec{\lambda}) = \pm \langle \xi, \eta | H_{kD} | \xi, \eta \rangle_{\pm}$. The energy surface can be written once more as

$$E_{k, \pm}^{\text{SAS}}(\vec{\lambda}) = \omega_A \mathcal{J}_{k, \pm}^{\text{SAS}}(\vec{\lambda}) + \Omega \left(\nu_{k, \pm}^{\text{SAS}}(\vec{\lambda}) + 1/2 \right) + \gamma \mathcal{I}_{k, \pm}^{\text{MF}}(\vec{\lambda}), \quad (31)$$

where the expectation values appearing in this expression (computed in the SAS) can be expressed as

$$\begin{aligned} \mathcal{J}_{k, \pm}^{\text{SAS}}(\vec{\lambda}) &= -j \cos \theta \frac{1 \pm (\cos \theta)^{2j-2} (-\cos \psi)^{2k}}{1 \pm (-\cos \theta)^{2j} (-\cos \psi)^{2k}}, \\ \nu_{k, \pm}^{\text{SAS}}(\vec{\lambda}) &= \frac{k-1/2}{2} \left[1 - \frac{\cos^2 \psi \pm (-\cos \theta)^{2j} (-\cos \psi)^{2k-2}}{1 \pm (-\cos \theta)^{2j} (-\cos \psi)^{2k}} \right], \\ \mathcal{I}_{k, \pm}^{\text{SAS}}(\vec{\lambda}) &= -2j \sqrt{\frac{2k}{N}} \sin \theta \sin \psi \cos \phi \cos \varphi \\ &\times \frac{1 \mp \tan \phi \tan \varphi (-\cos \theta)^{2j-1} (-\cos \psi)^{2k-1}}{1 \pm (-\cos \theta)^{2j} (-\cos \psi)^{2k}}. \end{aligned} \quad (32)$$

Now we have to minimize the energy surface (31) by requiring its derivative to be zero at the critical points $\vec{\lambda}_c^{\text{SAS}}$. This is a difficult task in this case mainly due to the intricate angular dependence of the above expectation values. However, as a first approximation, we may substitute the critical points $\vec{\lambda}_1^{\text{MF}}$ and $\vec{\lambda}_2^{\text{MF}}$ obtained for the mean field energy surface (12), a method we will refer to as the CSAS approach. Indeed, one can further verify that the critical point $\vec{\lambda}_1^{\text{MF}}$ is still a critical point of the SAS energy surface, i.e. $\vec{\lambda}_1^{\text{SAS}} = \vec{\lambda}_1^{\text{MF}}$. A simple calculation shows that the expectation value of the atomic relative population operator is

$$\mathcal{J}_{k, \pm}^{\text{CSAS}}(\gamma) = \begin{cases} -j \frac{1 \pm (-1)^{2k}}{1 \pm (-1)^{2(j+k)}}, & \text{for } |\gamma| < \gamma_c \\ -j \lambda^2 \frac{1 \pm (-1)^{2k} \lambda^{4(j-1)} \Gamma^k}{1 \pm (-1)^{2(j+k)} \lambda^{4j} \Gamma^k}, & \text{for } \gamma_c < |\gamma| < \gamma_m \end{cases}, \quad (33)$$

where $\Gamma \equiv 1 + \delta(\lambda^2 - \lambda^{-2})$, $\lambda \equiv \gamma_c/\gamma$ and $\delta \equiv \frac{j\omega_A}{\Omega(k-1/2)}$ are dimensionless parameters. In a similar fashion, we find that the expectation value of the photon number operator is $\nu_k^{\text{CSAS}}(\gamma) = 0$ for $|\gamma| < \gamma_c$, and

$$\nu_k^{\text{CSAS}}(\gamma) = \frac{k-1/2}{2} \left[1 - \frac{\Gamma \pm (-1)^{2(j+k)} \lambda^{4j} \Gamma^{k-1}}{1 \pm (-1)^{2(j+k)} \lambda^{4j} \Gamma^k} \right] \quad (34)$$

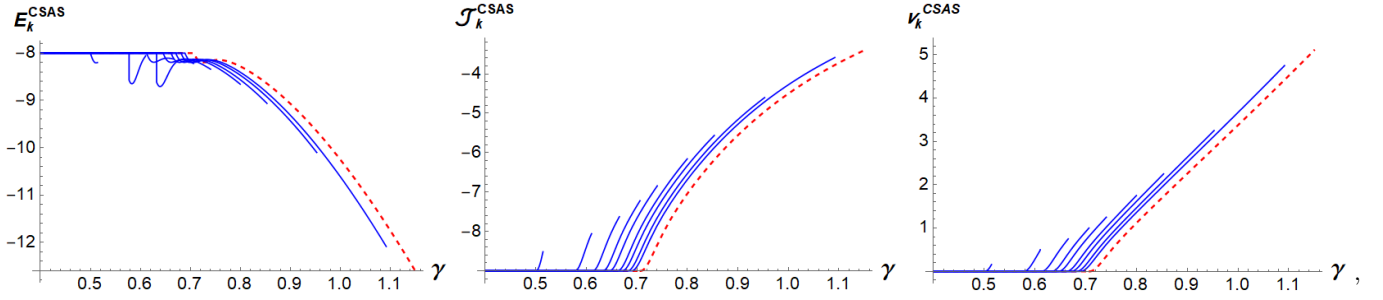


FIG. 2: Plot of the ground-state energy E_k^{CSAS} (left), the expectation value of the atomic relative population operator $\mathcal{J}_k^{\text{CSAS}}$ (center) and the expectation value of the analogue of the photon number operator ν_k^{CSAS} (right) as a function of the field-matter coupling γ , obtained using the MF critical points in the SAS expressions, for $k \in \{1, \frac{3}{2}, 2, \frac{5}{2}, 3, 4, 5, 7, 10\}$ (blue-continuous lines). As a benchmark, the red-dashed lines show these same quantities in the limiting case $k \rightarrow \infty$, which corresponds to the $\text{HW}(1) \otimes \text{SU}(2)$ Dicke model. All plots were obtained using $\omega_A = 1$, $\Omega = 2$, $N = 18$ and $j = 9$.

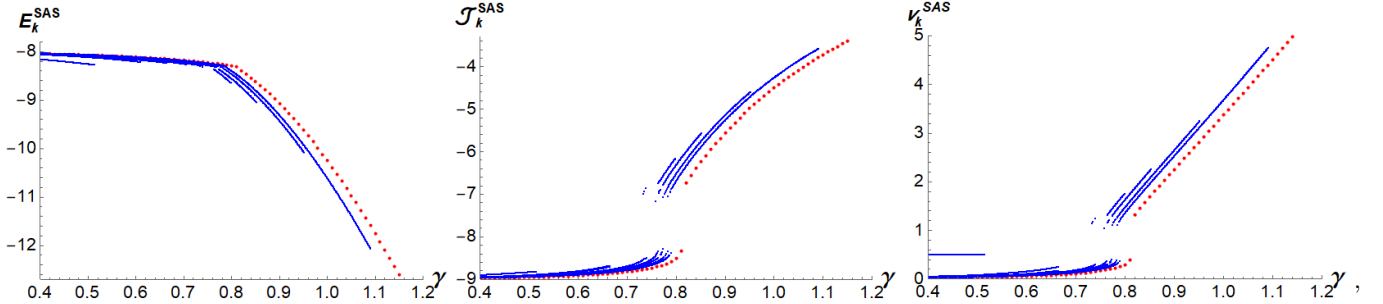


FIG. 3: Plot of the ground-state energy E_k^{SAS} (left), the expectation value of the atomic relative population operator $\mathcal{J}_k^{\text{SAS}}$ (center) and the expectation value of the analogue of the photon number operator ν_k^{SAS} (right) as a function of the field-matter coupling γ , obtained by numerically minimizing the SAS energy surface, for $k \in \{1, \frac{3}{2}, 2, \frac{5}{2}, 3, 4, 5, 7, 10\}$ (blue-continuous lines). As a benchmark, the red-dashed lines show these same quantities in the limiting case $k \rightarrow \infty$, which corresponds to the $\text{HW}(1) \otimes \text{SU}(2)$ Dicke model. All plots were obtained using $\omega_A = 1$, $\Omega = 2$, $N = 18$ and $j = 9$.

for $\gamma_c < |\gamma| < \gamma_m$.

From the above results we infer that the energy in the normal phase $|\gamma| < \gamma_c$ is a constant, namely

$$E_{k,\pm}^{\text{CSAS}}(\gamma) = \frac{\Omega}{2} - j\omega_A \frac{1 \pm (-1)^{2k}}{1 \pm (-1)^{2(j+k)}}. \quad (35)$$

In the usual Dicke model, the ground state of the system has an even parity for an integer j , as considered in [22], and an odd parity for a half-integer j . In the k -Dicke model, which is described by two interacting fermion fields, the parity of the ground state depends on both spins. For example, as we read from eq. (35), an even parity ground state with k and j both integers produces $-j\omega_A + \frac{\Omega}{2}$. However, the same result is obtained with an odd parity ground state with integer j and half-integer k .

The energy in the super-radiant phase $\gamma_c < |\gamma| < \gamma_m$

is

$$\begin{aligned} E_{k,\pm}^{\text{CSAS}}(\gamma) &= \frac{\Omega}{2} - j\omega_A \lambda^2 \frac{1 \pm (-1)^{2k} \lambda^{4(j-1)} \Gamma^k}{1 \pm (-1)^{2(j+k)} \lambda^{4j} \Gamma^k} \\ &+ \frac{\Omega}{2} (k - 1/2) \left[1 - \frac{\Gamma \pm (-1)^{2(j+k)} \lambda^{4j} \Gamma^{k-1}}{1 \pm (-1)^{2(j+k)} \lambda^{4j} \Gamma^k} \right] \\ &- \frac{j\omega_A}{\lambda^2} \frac{1 - \lambda^4}{1 \pm (-1)^{2(j+k)} \lambda^{4j} \Gamma^k}. \end{aligned} \quad (36)$$

In figure 2 we plot the ground state energy (at left), the expectation value of the atomic relative population operator (at middle) and the expectation value of the excitation number operator (at right), all for $N = 2j = 18$ (integer j) and $k \in \{1, \frac{3}{2}, 2, \frac{5}{2}, 3, 4, 5, 7, 10\}$, using the odd-parity ground state for $k = \frac{3}{2}, \frac{5}{2}$ and the even-parity ground state for $k = 1, 2, 3, 4, 5, 7, 10$. It can be observed that the behavior of the analyzed quantities is slightly different from the mean-field expressions in equations (23), (24) and (25). Mainly, the energy plot shows an oscillatory-like behavior near the transition, with a higher amplitude for the odd-parity case. In general, all quantities appear to have a smoother transition than its analogous mean-field plots in figure 1.

Another way to approximate the ground state of the

system is to numerically minimize the SAS energy surface in eq. (31). This approach has the disadvantage of not letting us have analytical expressions for the energy, the expectation value of the atomic relative population operator and the expectation value of the excitation number operator, nevertheless it allows us to have a better understanding of the behavior of these quantities in the normal region, where the MF and CSAS expressions have a constant value.

In figure 3 we plot the ground state energy (at left), the expectation value of the atomic relative population operator (at middle) and the expectation value of the excitation number operator (at right), obtained by numerically minimizing the SAS energy surface in eq. (31), all for $N = 2j = 18$ and $k \in \{1, \frac{3}{2}, 2, \frac{5}{2}, 3, 4, 5, 7, 10\}$. As in the CSAS approach, we use the odd-parity ground state for $k = \frac{3}{2}, \frac{5}{2}$ and the even-parity ground state for $k = 1, 2, 3, 4, 5, 7, 10$. It can be noticed from this plots that the transition looks less smooth, being obvious for the expectation values of the atomic relative population operator and the excitation number operator, as its graphs become discontinuous. The behavior in the normal region is also different from the one shown in figures 1 and 2, slightly changing instead of having a constant value. Another interesting thing to observe is the graph of the expectation value of the excitation number operator for $k = 1$, as it has a constant value of $\frac{1}{2}$, a completely different behavior than the one shown for all the used approaches and values of k .

It is worth mentioning that the cut-off value of the field-matter coupling used in both figure 2 and figure 3, is the same as in eq. (22), i.e. the same as in the mean-field case.

V. EXACT QUANTUM SOLUTION

For the exact quantum solution we resort to numerical diagonalization of the Hamiltonian and use the lowest eigenstate to compute the expectation value of the relevant observables. Across a quantum phase transition, the ground state of a system suffers a sudden, drastic change between neighboring states near the transition point. Thus it is natural to use the fidelity to detect the QPT in the exact quantum solution.

For a pure quantum state $|\psi\rangle$, the fidelity is defined as

$$\mathcal{F} = |\langle \psi(\gamma) | \psi(\gamma + \delta\gamma) \rangle|^2, \quad (37)$$

and it measures the overlap between the state at γ and the state at $\gamma + \delta\gamma$ [31]. At the transition point we expect a drop in the fidelity up to a minimum value.

In figure 4 we plot the fidelity between neighboring states as a function of the field-matter coupling γ , as defined in eq. (37). The blue lines correspond to the fidelities for different values of k , increasing from left to right, and the gray-continuous vertical lines indicate the corresponding transitions points characterized by the minimum value of the fidelity. The vertical red-dashed line

indicates the transition point in the usual Dicke model, also characterized by the minimum value of its corresponding fidelity [22]. Clearly, the drop in the fidelity is going towards the usual Dicke result as increasing k , as it should be.

By means of numerical diagonalization of the model Hamiltonian (9) and the fidelity between neighboring states in eq. (37), we have already proven the existence of a phase transition in the k -Dicke model. Now we analyze how the quantum expectation values of some physical quantities relevant to the system behaves near the transition point. In figure 5 we show the exact ground-state energy (at left), the expectation value of the atomic relative population operator \mathcal{J}_k (at center) and the photon number operator ν_k (at right), as a function of the field-matter coupling γ for a given value of j and different values of k . The red dashed lines correspond to the expectation values in the exact quantum solution of the Dicke Hamiltonian. We see from these plots that the quantum solution does indeed change in the normal region, as predicted by the numerically minimized SAS energy surface plots in figure 3, even though the transition is smoother, which can also be seen from the small ($\approx 10^{-5}$) drop of the fidelity in figure 4.

It is worth mentioning that the cut-off value of the field-matter coupling used in figure 5, is the same as in eq. (22), i.e. the same as in the mean-field case. This cause the blue-continues lines to go beyond its permitted values, even surpassing the Dicke graph, allowing us to infer that the real cut-off value of the field-matter coupling is less than γ_m in eq. (22).

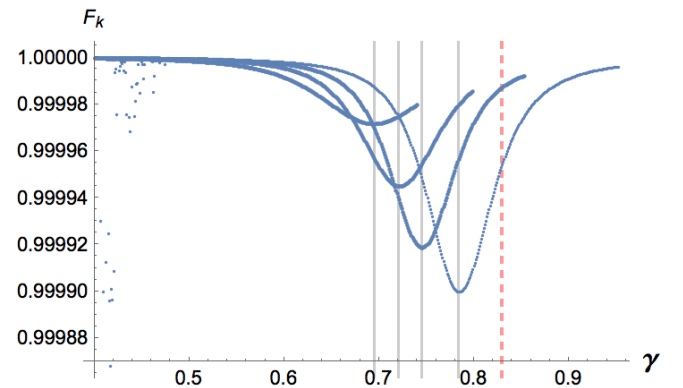


FIG. 4: Fidelity (blue lines) between neighboring states as a function of the field-matter coupling γ , obtained using the numerical diagonalization of the Hamiltonian. The vertical lines indicate the transition points characterized by the minimum value of the fidelity, for $k \in \{3, 4, 5, 7\}$ from left to right. The vertical red-dashed line corresponds to the transition point in the usual Dicke model, also obtained via numerical means and characterized by the minimum value of its corresponding fidelity.

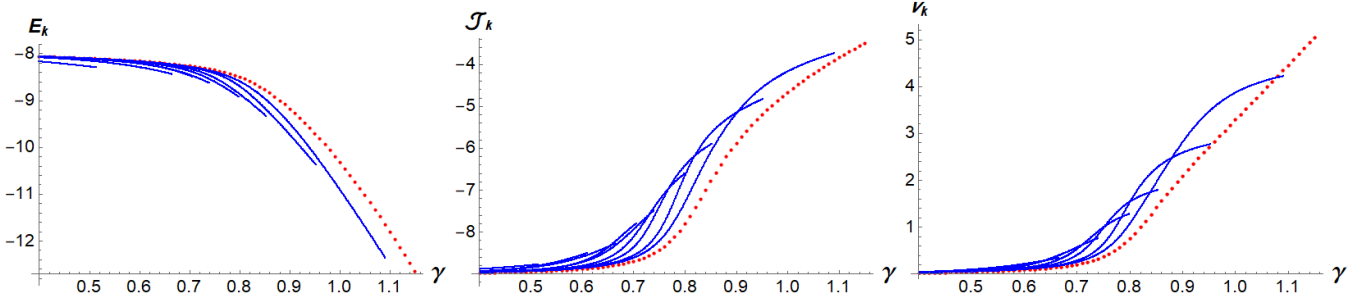


FIG. 5: Plot of the ground-state energy E_k (left), the expectation value of the atomic relative population operator \mathcal{J}_k (center) and the expectation value of the analogue of the photon number operator ν_k (right) as a function of the field-matter coupling γ , obtained by numerically diagonalizing the Hamiltonian, for $k \in \{1, \frac{3}{2}, 2, \frac{5}{2}, 3, 4, 5, 7, 10\}$ (blue-continuous lines). As a benchmark, the red-dashed lines show these same quantities in the limiting case $k \rightarrow \infty$, which corresponds to the $\text{HW}(1) \otimes \text{SU}(2)$ Dicke model. All plots were obtained using $\omega_A = 1$, $\Omega = 2$, $N = 18$ and $j = 9$.

VI. SUMMARY AND CONCLUSIONS

Motivated by the search of field theories incorporating a natural energy cutoff (which could alleviate the corresponding UV divergences, in principle), in this paper we have examined a group theoretical extension of the Dicke model which describes the interaction between N two-level identical atoms and a finite radiation field. The basis of our model is that the Heisenberg-Weyl group $\text{HW}(1)$, which is the one associate with the $\text{U}(1)$ electromagnetic field, can be obtained by the contraction of the $\text{SU}(2)$ group. Therefore, in a definite unitary irreducible representation k of the $\text{SU}(2)$ algebra, we built up raising and lowering spin operators which reduces to the usual bosonic creation and annihilation operators in the large k -representation limit. Interestingly, the corresponding k -oscillator model exhibits the main properties of the Kerr-like medium, and its main attribute is that it possesses a maximum number of excitations. By coupling a system of N two-level identical atoms with this finite radiation field we obtained the k -Dicke model.

The most relevant feature of the Dicke model is perhaps the presence of a phase transition between the normal and the super-radiant behavior, which is indeed sensitive to the properties of the radiation field. In this sense, such a phase transition should be affected by the coupling with a finite radiation field in the k -Dicke model. This is precisely what we tackled in this paper. By using the energy surface minimization method, which consists of minimizing the expectation value of the Hamiltonian in some trial variational state, we found that the k -Dicke model exhibits a quantum phase transition at a (k -dependent) critical value for the field-matter coupling strength $\gamma_c(k)$. The system then transits from the normal phase, for γ below the critical value $\gamma_c(k)$, to a super-radiant phase, for $\gamma_c(k) < \gamma < \gamma_m(k)$. Here, $\gamma_m(k)$ is the maximum value that the field-matter coupling strength can take, and it is a direct consequence of the maximum number of excitations in the system. Our analysis was carried out via three methods: through mean-field analysis (i.e. by using $\text{SU}(2) \otimes \text{SU}(2)$ coherent states), by

using parity-preserving symmetry-adapted states (using the critical values obtained in the mean-field analysis and numerically minimizing the energy surface) and by means of the exact quantum solution (i.e. by numerically diagonalizing the Hamiltonian).

We find that both, mean-field and symmetry-adapted analysis, when using the same critical values, exhibit a quantum phase transition, and the relevant observables have a similar behavior as functions of the field-matter coupling parameter, mainly a constant value in the normal region. The symmetry-adapted analysis, performed by numerically diagonalizing the energy surface, show a better resemblance to the exact quantum solution, in both the behavior of the observables in the normal region and the location of the transition, which was characterized for the exact solution by the minimum value of the fidelity between neighboring states. In all cases the respective Dicke solution was obtained in the limit $k \rightarrow \infty$, which corresponds to the $\text{HW}(1) \otimes \text{SU}(2)$ model.

We close by commenting the possible connection between the algebraic model we have considered and the q -bosons. The anharmonic q -bosons are defined by the following commutation relations [32, 33]

$$[a_q, a_q^\dagger] = q^{n_q}, \quad [n_q, a_q] = -a_q, \quad [n_q, a_q^\dagger] = a_q^\dagger, \quad (38)$$

where the deformation parameter q is in general a complex number. This algebra, which is usually referred as Heisenberg-Weyl q -algebra and denoted by HW_q , defines a special deformation scheme of the usual harmonic-oscillator algebra (3), to which it is reduced in the limit $q \rightarrow 1$. It has been useful in the description of anharmonic vibrations of diatomic molecules and solids, since the corresponding oscillator-like model exhibits the main features of the Morse oscillator. Our k -oscillator algebra (6) may be obtained from the q -bosons (38) for real values of q approaching to one from below. To see this, let $q < 1$ and $p = \frac{1}{1-q}$, so that $q = 1 - \frac{1}{p}$. Then we have

$$q^{n_q} = \left(1 - \frac{1}{p}\right)^{n_q}. \quad (39)$$

The harmonic limit is recovered for $p \rightarrow \infty$ in this parametrization. Further, assuming that $(1/p) \ll 1$, we can Taylor expand the above result to obtain

$$q^{n_q} \approx 1 - \frac{n_q}{p} + \frac{1}{2} \frac{n_q(n_q - 1)}{p^2} + \mathcal{O}(p^{-3}). \quad (40)$$

If we now substitute the leading terms (up to order $1/p$) in the q -bosons algebra (38) and we identify the parameter p with k , n_q with n_k and the creation and annihilation operators a_q, a_q^\dagger with b_k, b_k^\dagger , we recover the SU(2) algebra (6). We mention in passing that, if q approaches to one from above, we can define the new parameter $r = \frac{1}{q-1}$ and the approximation equivalent to eqs. (39) and (40) leads to the non-compact SU(1, 1) algebra. In summary:

$$\lim_{q \rightarrow 1-0^+} \text{HW}_q \rightarrow \text{SU}(2), \quad \lim_{q \rightarrow 1+0^+} \text{HW}_q \rightarrow \text{SU}(1, 1). \quad (41)$$

Although the q -bosons algebra contracts to the SU(2) algebra, it is not clear that their representations also match in the limit. This can be seen from the fact that the SU(2) algebra is naturally defined in a finite Hilbert space, while the q -algebra can be defined in a finite-dimensional representation only when q is a nontrivial root of the equation $q^{n_q} = 1$ [34]. A possible extension of this work must be then the analysis of the quantum phase transition in the q -Dicke model.

Acknowledgments

L. F. Quezada thanks C3-UNAM for financial support. A. Martín-Ruiz and A. Frank acknowledge support from CONACYT under project No. 012277.

[1] M. Visser, Phys. Rev. D **80**, 025011 (2009).
[2] R. H. Dicke, Phys. Rev. **93**, 99 (1954).
[3] K. Hepp and E. H. Lieb, Phys. Rev. A **8**, 2517 (1973).
[4] K. Hepp and E. H. Lieb, Ann. Phys. **76**, 360 (1973).
[5] Y. K. Wang and F. T. Hioe, Phys. Rev. A **7**, 831 (1973).
[6] K. Baumann, C. Guerlin, F. Brennecke and T. Esslinger, Nature (London) **464**, 1301 (2010).
[7] D. Nagy, G. Kónya, G. Szirmai and P. Domokos, Phys. Rev. Lett. **104**, 130401 (2010).
[8] V.K. Dobrev, *Quantum Algebras: Representations and Real Forms*. In: Gruber B. (eds) Symmetries in Science VI. Springer, Boston, MA (1993).
[9] M. Chaichian, D. Ellinas and P. Kulish, Phys. Rev. Lett. **65**, 980 (1990).
[10] D. Bonatsos, C. Daskaloyannis and G. A. Lalazissis, Phys. Rev. A **47**, 3448 (1993).
[11] J. Črnugelj, M. Martinis and V. Mikuta-Martinis, Phys. Rev. A **50**, 1785 (1994).
[12] O. de los Santos-Sánchez and J. Rcamier, J. Phys. B: At. Mol. Opt. Phys. **45**, 015502 (2012).
[13] O. de los Santos-Sánchez, J. Phys. A: Math. Theor. **51**, 305303 (2018).
[14] F. Ricci, Monatsh. Math. **101**, 211 (1986).
[15] S. M. Chumakov, A. Frank and K. B. Wolf, Phys. Rev. A **60**, 60 (1999).
[16] A. Martín-Ruiz, A. Frank and L. F. Urrutia, Phys. Scr. **89**, 045103 (2014).
[17] O. Castaños, R. López-Peña, E. Nahmad-Achar, J. G. Hirsch, E. López-Moreno, and J. E. Vitela, Phys. Scr. **79**, 065405 (2009).
[18] O. Castaños, E. Nahmad-Achar, R. López-Peña, and J. G. Hirsch, Phys. Scr. **80**, 055401 (2009).
[19] O. Castaños, E. Nahmad-Achar, R. López-Peña, and J. G. Hirsch, Phys. Rev. A **83**, 051601 (2011).
[20] O. Castaños, E. Nahmad-Achar, R. López-Peña, and J. G. Hirsch, Phys. Rev. A **86**, 023814 (2012).
[21] J. G. Hirsch, O. Castaños, E. Nahmad-Achar, and R. López-Peña, Phys. Scr. **T153**, 014033 (2013).
[22] L. F. Quezada and E. Nahmad-Achar, Phys. Rev. A **95**, 013849 (2017).
[23] S. Cordero, R. López-Peña, O. Castaños and E. Nahmad-Achar, Phys. Rev. A **87**, 023805 (2013).
[24] S. Cordero, O. Castaños, R. López-Peña and E. Nahmad-Achar, E. J. Phys. A **46**, 505302 (2013).
[25] S. Cordero, E. Nahmad-Achar, R. López-Peña and O. Castaños, Phys. Rev. A **92**, 053843 (2015).
[26] S. Cordero, O. Castaños, R. López-Peña and E. Nahmad-Achar, Phys. Rev. A **94**, 013802 (2016).
[27] L. F. Quezada and E. Nahmad-Achar, Phys. Rev. A **97**, 063819 (2019).
[28] F. T. Arecchi, E. Courtens, R. Gilmore and H. Thomas, Phys. Rev. A **6**, 2211 (1972).
[29] K. Wódkiewicz and J. H. Eberly, J. Opt. Soc. Am. B **2**, 458 (1985).
[30] O. Castaños, E. Nahmad-Achar, R. López-Peña and J. G. Hirsch, Phys. Rev. A **84**, 013819 (2011).
[31] P. Zanardi and N. Paunkovic, Phys. Rev. E **74**, 03123 (2006).
[32] L. C. Biedenharn, J. Phys. A: Math. Gen. **22**, L873 (1989).
[33] A. J. Macfarlane, J. Phys. A: Math. Gen. **22**, 4581 (1989).
[34] M. Angelova and A. Frank, J. Phys. A: Math. Gen. **34**, L503 (2001).